Spring 3-1-1981

Dielectric Line Coupler Using Only Curved Sections

M Abouzahra
University of Colorado Boulder

L Lewin
University of Colorado Boulder

DIELECTRIC LINE COUPLER USING ONLY CURVED SECTIONS

by

M. Abouzahra and L. Lewin

Scientific Report #61

March 1981

Electromagnetics Laboratory
Department of Electrical Engineering
University of Colorado
Boulder, Colorado 80309

This research was supported by the National Bureau of Standards (NBS) under grant no. NB 79 RAC 90009.

TABLE OF CONTENTS

LIST OF FIGURES

DIELECTRIC LINE COUPLER USING ONLY CURVED SECTIONS

M. Abouzahra and L. Lewin

Abstract

The differential equations of a single section curved coupler are solved. From its solutions, the reverse coupling (directivity) and reflection are derived and found to be exponentially small. The fields on both lines are found to be closely in quadrature. The attenuation formulas of the transmission losses (dielectric, wall, and radiation) are quoted. A numerical example of a 3 dB coupler, centered at 94 GHZ, is demonstrated.

I. Introduction

The problem of wave propagation in a parallel plane waveguide partially filled with dielectric (which is also referred to as H-Guide or Duo-dielectric parallel plane waveguide) has been investigated and reported on by many authors[1-10].

Coupled-wave theory[11-13] has been applied to the solution of a variety of waveguide problems. Recently, the theory of coupling between parallel transmission lines was extended to describe the coupling between curved transmission lines[14-18].

It is the purpose of this report to discuss further work on coupling between curved transmission lines, namely two curved rectangular dielectric waveguides, with no linear sections, sandwiched between two parallel perfectly conducting plates (see Fig. 1). The intention of not using straight sections is to avoid the reflection coming from the discontinuity between the straight and curved parts and to enable the coupling to be increased, thus giving more bandwidth. A continuously curved section should exhibit reflection of a smaller magnitude. We will present further information on the dependence of coupling on the dimensional parameters such as width, height, line spacing, and dielectric constant. A suitable choice of the dimensional parameters of a 3 dB coupler with emphasis on broad-band coupling, minimum reflection, reduced reverse coupling, and reasonable losses (dielectric, wall, and radiation losses) is recommended.

The structure shown in Fig. 1 is capable of supporting both TE and hybrid modes[8,19]. An analytical description for the fields of the symmetrical TE even mode (dominant mode) has been reported on in Rept. No. 49. The field distribution for the antisymmetric TE_0 even

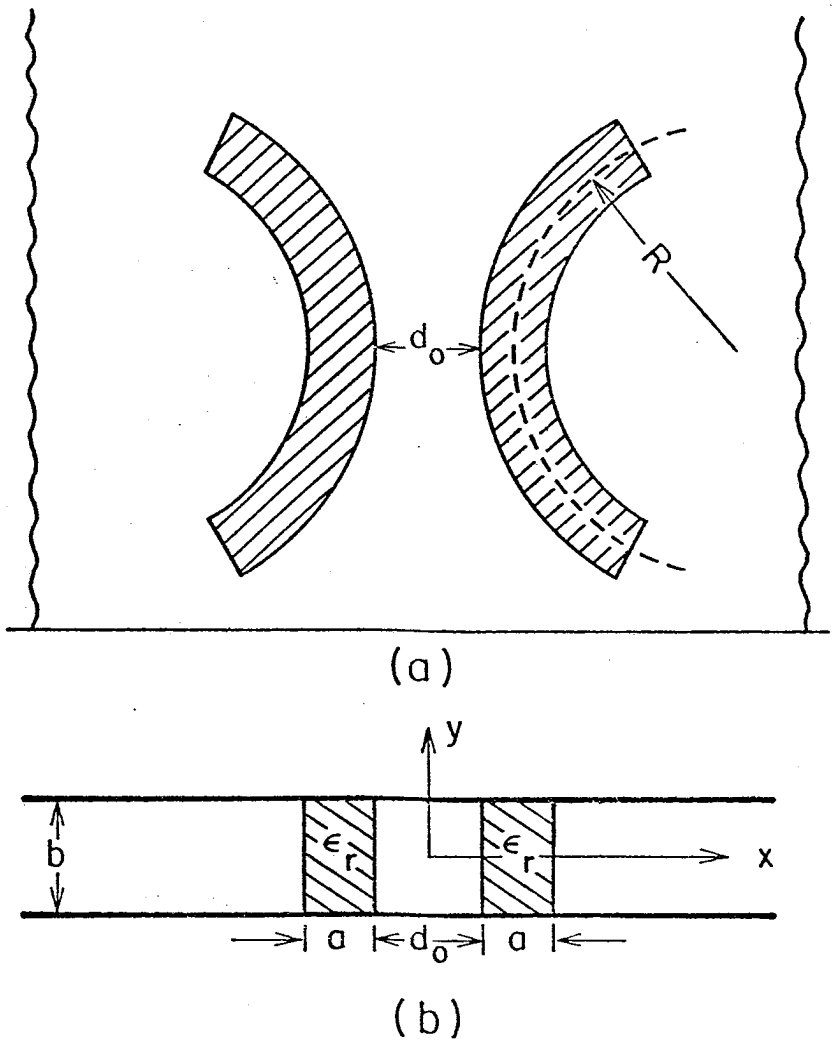

Fig. 1 (a) Top view of a 3 dB curved dielectric directional coupler.
(b) Cross section of the parallel plane waveguide partially filled with two curved slabs separated by a distance d_o.
The positive z-axis is out of the paper.

mode can be easily obtained when replacing cos (py) by sin (py), and sin (py) by - cos (py), in the field expressions of symmetrical mode. The field expressions for the symmetric $H_x = 0$ mth rank hybrid modes, for both single line and two coupled lines, is presented. Feeding the coupler by the first order $H_x = 0$ hybrid mode, symmetrical and antisymmetrical excitations, is found to give a relatively poor 3-dB bandwidth. Because of time pressure it has not been possible to study the perturbation due to the channel-guide structure on the propagation parameters.

II. Summary of Methods and Results

The geometry of the proposed 3 dB dielectric directional coupler is shown in Fig. 2. The structure as shown is composed of two continuous curved sections. The field amplitude differential equations (of the actual modes) are written down, and due to the appearance of a z-dependent exponential term (in the differential equations) no exact closed form solution is available. As a result, two completely different approximate methods are used. From the first method, which is an iterative technique, it was mathematically difficult to extract a complete accurate solution. However, we were able to derive accurate expressions for the reflection coefficient and the directivity, and hence to conclude that they are exponentially small and can be neglected. Bearing in mind this beneficial result, a second approach is employed and found to give a complete and accurate solution for the forward field amplitudes (propagating on both lines). No reflected wave terms appear in this solution. This is because the amplitude of the

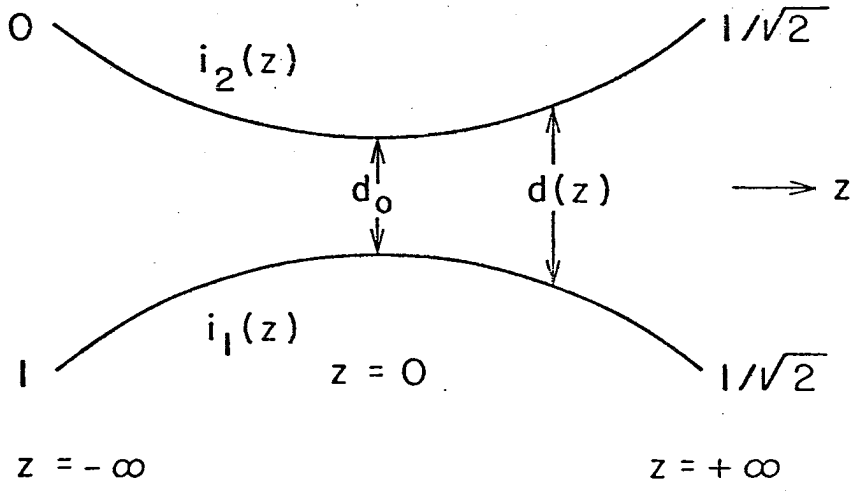

Fig. 2 Geometry and boundary conditions of the 3 dB coupler.

reflected wave is known to be exponentially small and hence is lost in the power series arising from this method. A constant phase difference of 90^{o} is found to exist between the fields of both guides. By imposing the 3 dB design requirements (of the directional dielectric coupler) the design parameters are calculated. The transmission losses (radiation, dielectric and wall losses) are calculated using approximate attenuation formulas derived by other authors. The transmission losses arising from the walls and the dielectrics are of small order (10^{-2} and 10^{-3} neper/cm respectively). The radiation losses are found to be larger than -50 dB when the minimum radius of curvature R is less than 15 mm. Finally, the field amplitudes of both guides are plotted versus frequency with 94 GHz as design frequency. Figs. 3 and 4 illustrate the coupler performance (when it is fed by a TE_0 mode) as a function of frequency, separation d_0, guide width, and the relative dielectric constant of the filling material. It is quite clear, from these graphs, that the guide width and the relative dielectric constant have only minor effect on the coupler performance. The separation distance d_0 (which is proportional to R , the minimum radius of curvature) is found to have a large effect on the coupler band-width. The smaller the separation, the stronger the coupling and hence the larger the bandwidth. However, the separation distance d_0 (and hence R) cannot be decreased below a certain value (corresponding to R = 15 mm) otherwise the radiation becomes excessive. Fig. 5 shows the frequency performancy of a 3-dB directional coupler fed by the $H_x = 0$ hybrid mode. The 3 dB bandwidth compared to the first case (20 GHz), is found to be smaller and hence of less practical use. A suitable choice of a 3 dB TE_0 dielectric

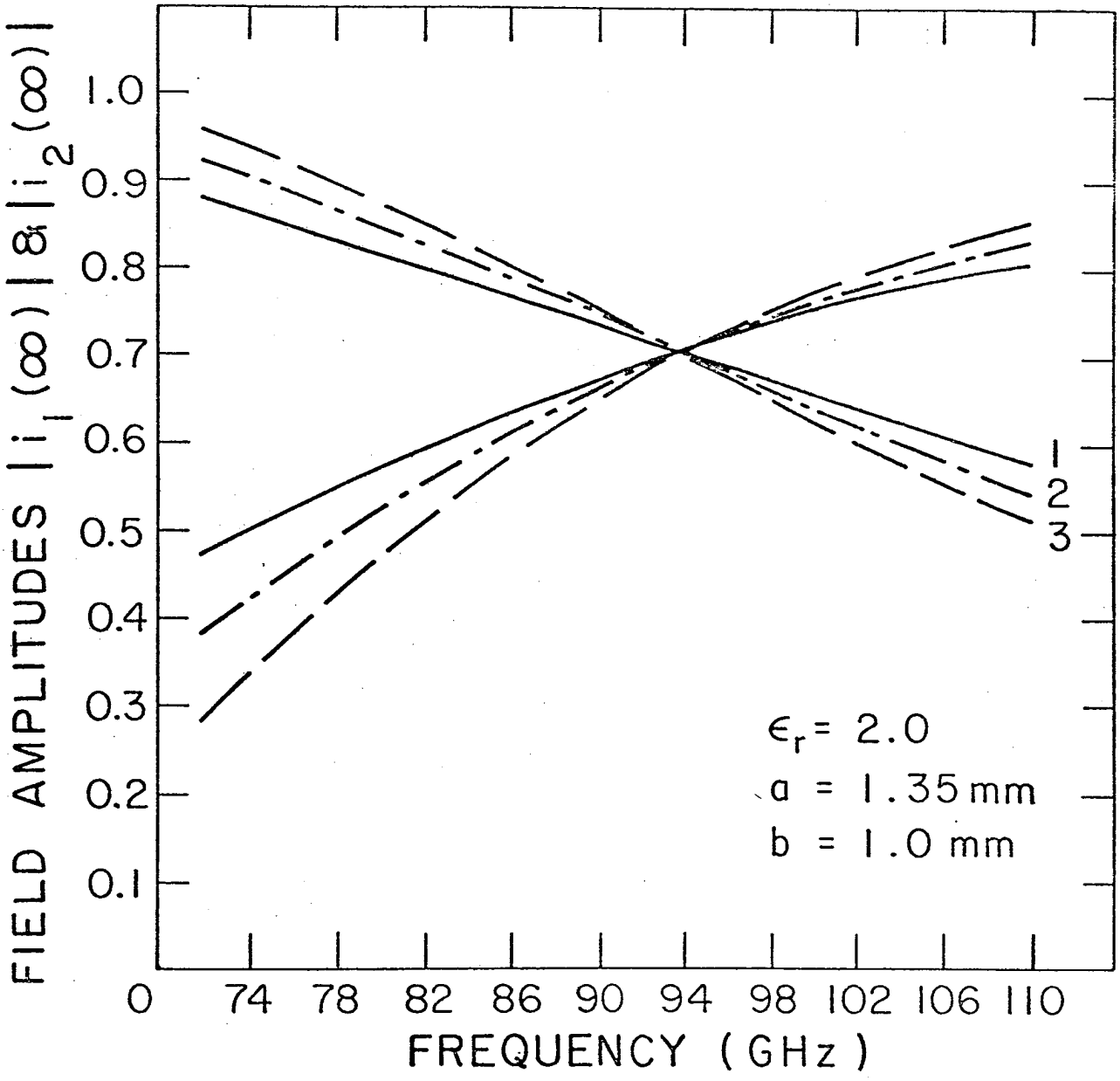

	d_o (mm)	B.W. (GHz)	R (mm)	CURVATURE RAD. (dB)	L (mm)
1 ———	0.2	30	7	-22	1.7
2 —·—	0.4	23	13	-37	3.2
3 — —	0.6	19	23.5	-75	5.3

Fig. 3 Field amplitudes of TE_0 mode versus frequency (94 GHz, design frequency).

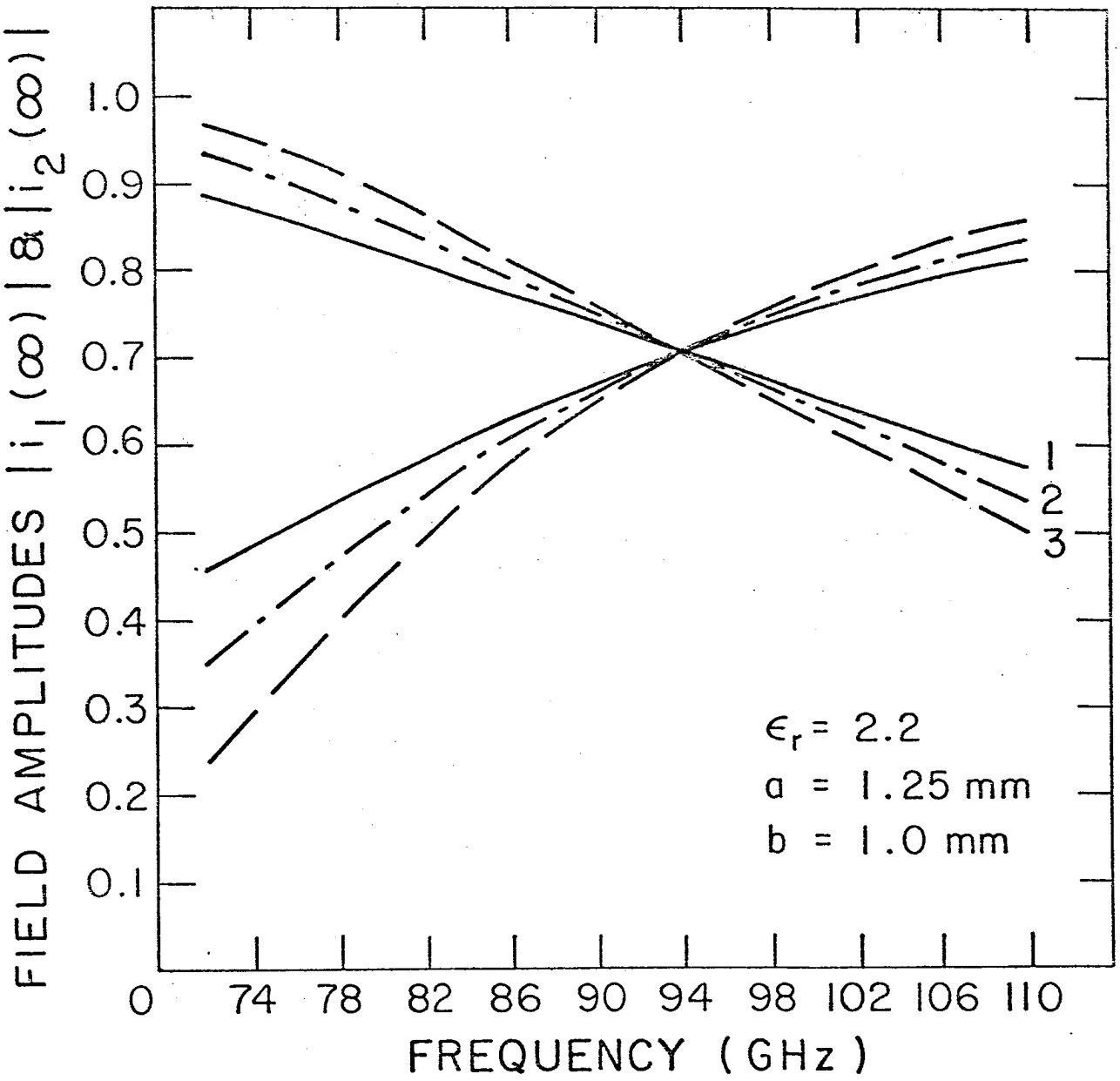

	d_o (mm)	B.W. (GHz)	R (mm)	CURVATURE RAD. (dB)	L (mm)
1 ———	0.2	29	6.4	-25	1.6
2 —·—	0.4	21	12.35	-48	3.2
3 — —	0.6	19	24	-90	5.4

Fig. 4 Field amplitudes of TE_o mode versus frequency (94 GHz, design frequency).

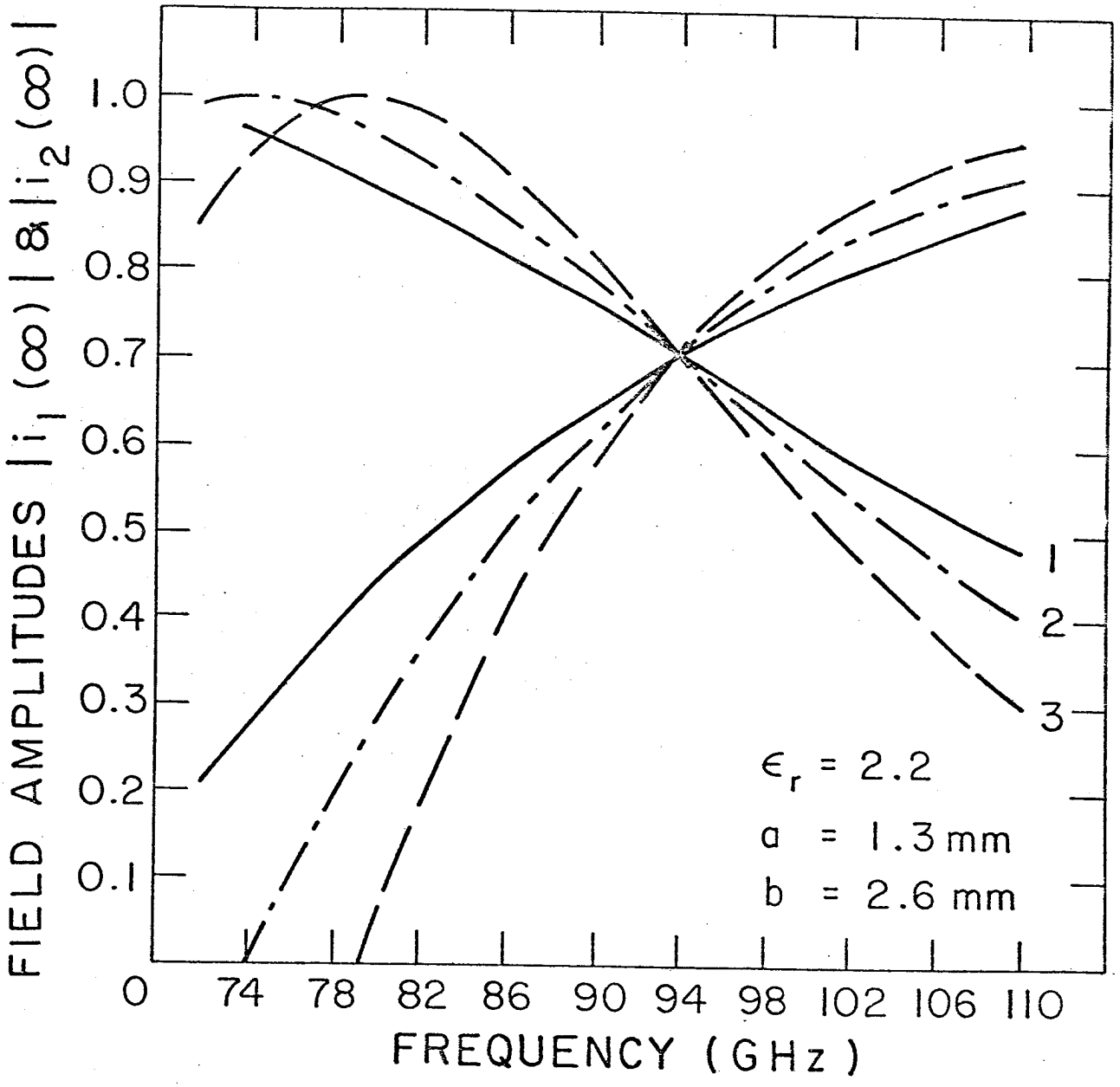

	d_o (mm)	B.W. (GHz)	L (mm)
1 ———	0.2	16	1.36
2 —·—	0.4	12	3.0
3 — —	0.6	9	6.0

Fig. 5 Field amplitudes of the lowest order $H_x = 0$ mode versus frequency (94 GHz design frequency).

directional coupler dimension is

$$a = 1.35 \text{ mm}$$

$$b = 1 \text{ mm}$$

$$\varepsilon_r = 2$$

$$R = 15 \text{ mm}$$

For this specific choice, the 3 dB bandwidth is 20 GHz and the reflection coefficient and directivity are extremely small (the calculation indicates -200 dB, but is not accurate at this minute level).

III. Analysis

The geometry and the coordinate system are shown in Fig. 2. The structure to be analyzed consists of two parabolic slabs of width a and height b separated by a distance $d(z)$ given by

$$d(z) = d_0[1+(\frac{z}{L})^2] \tag{1}$$

The minimum radius of curvature of each line is R. The bending loss of the dielectric waveguide consists only of the radiation loss from the curved section. Conversion loss due to discontinuity at junctions is avoided. In this analysis we will use the field amplitude differential equations that were derived in report no. 52 (and/or eqs. (13) of Ref [17]), for the curved section, rewritten as

$$\frac{d^2I}{dz^2} + \beta_o^2 I = -2\beta_o \Delta\beta I \delta(z) \qquad (2\text{-a})$$

$$\frac{d^2i}{dz^2} + \beta_o^2 i = 2\beta_o \Delta\beta i \delta(z) \qquad (2\text{-b})$$

$$\frac{d^2V}{dz^2} + \beta_o^2 V = -2\beta_o \Delta\beta V \delta(z) \qquad (2\text{-c})$$

$$\frac{d^2v}{dz^2} + \beta_o^2 v = 2\beta_o \Delta\beta v \delta(z) \qquad (2\text{-d})$$

where

$$\delta(z) = e^{-h_o d_o (\frac{z}{L})^2} \qquad (3)$$

and $\frac{d_o}{L^2}$ corresponds to $2c$ in report no. 52 (where c is half the inverse of the radius of the curved section, i.e. $c = \frac{1}{2R}$). In this new scheme of notation d_o represents the separation between the two lines at $z = 0$, L is the longitudinal distance at which the separation distance is doubled, (I,V) and (i,v) stand respectively for the symmetrical and the antisymmetrical modes, β_o is the propagation contstant (of the propagating mode) for a single linear line in isolation, and $\Delta\beta$ is the shift in propagation constant due to the coupling. The value of $\Delta\beta$ when the coupler is supporting the TE mode was given earlier [10]. In appendix A, the field expressions as well as the value of $\Delta\beta$ for the $H_x = 0$ lowest order hybrid mode are presented. Finally h_o of eq. (3) represents the transverse propagation constant in the air region. The z- dependent exponential term that appears on the right hand sides of (2-a) through (2-d) is because of the variable coupling along the curved lines of the coupler.

As a result of the z-dependent term, there is no exact closed form solution for these differential equations and hence an approximate iteration method will be employed. A full detailed analysis of two different iterative methods are given in the appendix.

1. First method

The full details of this method are demonstrated in appendix B. The employment of the variation of parameters technique followed by iteration, in this method, is found to give the coupled field amplitudes as,

$$i_1(\infty) = e^{-j\beta_o z}\left[1 - (\Delta\beta)^2\left\{\frac{\pi}{2\alpha}\left(1 + e^{-2\beta_o^2/\alpha}\right) - j\,\frac{\sqrt{\pi}}{\alpha}\,\mathrm{Daw}\left(\beta_o\sqrt{\frac{2}{\alpha}}\right)\right\} + \hat{A}\,(\Delta\beta)^4\right] + O(\Delta\beta)^6 \tag{4}$$

$$i_2(\infty) = -\,j\,e^{-j\beta_o z}\,\Delta\beta\sqrt{\frac{\pi}{\alpha}}\left[1 - (\Delta\beta)^2\,\frac{\pi}{6\alpha}\,\{1 + \hat{J}_1 + \hat{J}_2\}\right] + O(\Delta\beta)^5 \tag{5}$$

where

$$\alpha = \frac{h_o d_o}{L^2} \tag{6}$$

$$\hat{J}_1 = 6\sqrt{\frac{3}{\pi}}\;e^{-2\beta_o^2/\alpha}\int_o^{\infty} e^{-3\left(x + j\beta_o\sqrt{\frac{2}{3\alpha}}\right)^2}\,[1 + \mathrm{erf}(x)]\,dx \tag{7}$$

$$\hat{J}_2 = 3\sqrt{\frac{3}{\pi}}\ e^{-2\beta_o^2/\alpha} \int_o^\infty e^{-3(x + j\frac{\beta_o}{\sqrt{6\alpha}})^2}\ \mathrm{erfc}\left[x + j\beta_o\sqrt{\frac{3}{2\alpha}}\right] dx \tag{8}$$

$$\mathrm{Daw}(x) = e^{-x^2} \int_o^x e^{t^2}\, dt$$

$$\mathrm{erf}(x) = \frac{2}{\sqrt{\pi}} \int_o^x e^{-t^2}\, dt \tag{9}$$

$$\mathrm{erfc}(x) = 1 - \mathrm{erf}(x)$$

$$\mathrm{Re}(\hat{A}) = \frac{\pi^2}{6\alpha^2}\left[1 + \mathrm{Re}\{\hat{J}_1 + \hat{J}_2\}\right] + \sqrt{\frac{\pi}{\alpha}}\, e^{-\beta_o^2/\alpha}\ \mathrm{Re}(\hat{S}) - \frac{1}{2}\left[|\hat{K}|^2 + |\hat{C}|^2\right] \tag{10}$$

$$\hat{K} = \frac{\pi}{2\alpha}\left(1 + 2\, e^{-2\beta_o^2/\alpha}\right) - j\,\sqrt{\frac{\pi}{\alpha}}\ \mathrm{Daw}\left(\beta_o\sqrt{\frac{2}{\alpha}}\right) \tag{11}$$

$$\hat{C} = \frac{\pi}{\alpha}\, e^{-\beta_o^2/\alpha} - j\ 2\sqrt{\frac{\pi}{\alpha}}\ e^{-\beta_o^2/2\alpha}\ \mathrm{Daw}\left(\frac{\beta_o}{\sqrt{2\alpha}}\right) \tag{12}$$

$$\hat{S} = \hat{J}_3 + \hat{J}_4 + \hat{J}_5 + \hat{J}_6 \tag{13}$$

$$\hat{J}_3 = \frac{\pi}{2\alpha}\sqrt{\frac{3}{\alpha}}\ e^{-\beta_o^2/\alpha} \int_o^\infty e^{-3x^2}\ \mathrm{erfc}\left[x + j\beta_o\sqrt{\frac{2}{3\alpha}}\right] dx$$

$$\hat{J}_4 = \frac{\pi}{2\alpha}\sqrt{\frac{3}{\alpha}}\ e^{-3\beta_o^2/\alpha} \int_o^\infty e^{-3\left[x + j\beta_o\sqrt{\frac{2}{3\alpha}}\right]^2} \left\{1 + \mathrm{erf}\left[x - j\beta_o\sqrt{\frac{2}{3\alpha}}\right]\right\} dx$$

$$\hat{J}_5 = \frac{\pi}{2\alpha}\sqrt{\frac{3}{\alpha}}\ e^{-\beta_o^2/\alpha} \int_o^\infty e^{-3\left[x + j\frac{\beta_o}{\sqrt{6\alpha}}\right]^2} \left\{1 + \mathrm{erf}\left[x - j\frac{\beta_o}{\sqrt{6\alpha}}\right]\right\} dx$$

$$\hat{J}_6 = \frac{\pi}{2\alpha}\sqrt{\frac{3}{\alpha}}\, e^{-\beta_o^2/\alpha} \int_0^\infty e^{-3\left[x - j\frac{\beta_o}{\sqrt{6\alpha}}\right]^2} \operatorname{erfc}\left[x - j\frac{\beta_o}{\sqrt{6\alpha}}\right] dx \tag{14}$$

Moreover, the reflection coefficient due to coupling as well as the reverse coupling (directivity) are found respectively, to be

$$\Gamma = -(\Delta\beta)^2\left[\frac{\pi}{\alpha}\, e^{-\beta_o^2/\alpha} - j\frac{2\sqrt{\pi}}{\alpha}\, e^{-\beta_o^2/2\alpha}\, \mathrm{Daw}\left(\frac{\beta_o}{\sqrt{2\alpha}}\right)\right] + o(\Delta\beta)^4 \tag{15}$$

$$D = -j\left[\Delta\beta\left\{\sqrt{\frac{\pi}{\alpha}}\, e^{-\beta_o^2/\alpha} - (\Delta\beta)^2\, \mathrm{Re}(\hat{S})\right\} - j(\Delta\beta)^3\, \mathrm{Im}(\hat{S})\right] + o(\Delta\beta)^5 \tag{16}$$

Neglecting terms involving $e^{-2\beta_o^2/\alpha}$, which is exponentially small, in Eqs (4) and (5) yields

$$i_1(\infty) \simeq e^{-j\beta_o z}\left[1 - (\Delta\beta)^2\frac{\pi}{2\alpha} + (\Delta\beta)^4\frac{\pi^2}{24\alpha^2}\right] + o(\Delta\beta)^6 \tag{17}$$

$$i_2(\infty) \simeq -j\, e^{-j\beta_o z}\left[\Delta\beta\sqrt{\frac{\pi}{\alpha}} - \frac{(\Delta\beta)^3}{6}\left(\frac{\pi}{\alpha}\right)^{3/2}\right] + o(\Delta\beta)^5 \tag{18}$$

Similarly, Γ and D are found to vanish when terms as $e^{-\beta^2_o/\alpha}$ are ignored. Hence, we may conclude that, due to the absence of the linear section in the coupler geometry, Γ and D are exponentially small and therefore can be neglected.

The three terms on the right hand side of equation (17) are the leading terms of the Taylor expansion of $\cos\left(\Delta\beta\sqrt{\frac{\pi}{\alpha}}\right)$. On the other

hand, the two terms on the right of Eq (18) are the leading terms of the Taylor expansion of $-j\sin(\Delta\beta\sqrt{\frac{\pi}{\alpha}})$.

Thus, once more [15-17], it is found that i_1 and i_2 are in quadrature, which is to be expected on general grounds.

By imposing the design requirement of a 3-dB coupler, i.e. $|i_1(\infty)|^2 = |i_2(\infty)|^2$, and using Eqs. (4) and (5), we get

$$1 - (\Delta\beta)^2 \frac{\pi}{\alpha}\left[2 + e^{-2\beta_o^2/\alpha}\right] + (\Delta\beta)^4\left\{\frac{2}{3}\frac{\pi^2}{\alpha^2}\left[1 + \mathrm{Re}\left\{\hat{J}_1 + \hat{J}_2\right\}\right] + 2\sqrt{\frac{\pi}{\alpha}}\, e^{-\beta_o^2/\alpha}\,\mathrm{Re}(\hat{S}) - |\hat{C}|\right\} = 0 \tag{19}$$

which upon neglecting the exponentially small terms reduces to

$$1 - 2(\Delta\beta)^2 \frac{\pi}{\alpha} + \frac{2}{3}(\Delta\beta)^4 \frac{\pi^2}{\alpha^2} = 0 \tag{20}$$

After solving Eq.(20), d_o and L will be obtained as follows:

$$(\Delta\beta)^2 = \frac{\alpha X}{\pi} \tag{21}$$

where x is a root of (20). We assume an exponential dependence of $\Delta\beta$ on the separation distance as

$$\Delta\beta = c_o\, e^{-h_o d_o} \tag{22}$$

where

$$c_o = \frac{p_o^2 \, h_o}{\beta_o k_o^2 (\varepsilon_r - 1) \left(\frac{a}{2} + \frac{1}{h_o}\right)} \qquad \text{For } TE_o \text{ mode}$$

$$= \frac{\varepsilon_r \, p_o^2 \, h_o}{\beta_o k_o^2 (\varepsilon_r - 1) \left[\frac{a}{2} + \frac{\varepsilon_r}{h_o} + \frac{a h_o^2}{2k_o^2} (\varepsilon_r + 1)\right]} \qquad \text{For } H_{x=o}^{(1)} \text{ hybrid mode (Appendix A)}$$

(23)

From (21) and (22) d_o becomes,

$$d_o = \frac{1}{2h_o} \ln \left[\frac{\pi c_o^2}{\alpha x}\right] \tag{24}$$

and upon using (6) we obtain,

$$L = \sqrt{\frac{h_o \, d_o}{\alpha}} \tag{25}$$

where x is approximately equal to $\left(\frac{\pi}{4}\right)^2$ and

$$\alpha = \frac{h_o}{R} \tag{26}$$

and R is the minimum radius of the curved section. Hence

$$L = \sqrt{R d_o} \tag{27}$$

At this point, we have already derived the design equations (24) and (27), and we may start plotting Eqs.(17) and (18) for the coupled field amplitudes. However, Equations (17) and (18) are not completely accurate. This is because $\Delta\beta\sqrt{\frac{\pi}{\alpha}}$ is large, and hence some more higher order terms in $\Delta\beta$ are needed to get exact representation of the sinusoidal functions. Due to the difficulty in proceeding further with this approach (though it is possible) another method is employed.

This alternative approach is explained in detail in Appendix C, and only its results will be presented in the next section.

2. Second Method

The basic advantage of the previous approach is the discovery that Γ and D are exponentially small. Bearing in mind this beneficial result, we are able to use an alternative procedure to solve the differential Equations (2-a) through (2-d). The detail of this method is included in Appendix C. The amplitudes of the actual coupled fields are found to be

$$i_1(\infty) = e^{-j\beta_o z} e^{j\frac{\Delta\beta^2}{2\beta_o}\sqrt{\frac{\pi}{2\alpha}}} \operatorname{Cos}\left[\Delta\beta\sqrt{\frac{\pi}{\alpha}}\right] \tag{28}$$

$$i_2(\infty) = -je^{-j\beta_o z} e^{j\frac{\Delta\beta^2}{2\beta_o}\sqrt{\frac{\pi}{2\alpha}}} \operatorname{Sin}\left[\Delta\beta\sqrt{\frac{\pi}{\alpha}}\right] \tag{29}$$

From Eqs. (28) and (29) we learn that a constant phase difference of 90° exists between the two guides. We also find that the phase of the guide in which the power is increasing will always lag 90° behind the phase of the guide in which the power is decreasing. Physically, the reason for this phase difference is the necessary phase relation between the polarization (caused by the field in guide 1), and the field in guide 2 if power is to be generated in guide 2[22].

On the other hand, no reflected terms appear in the expressions of i_1 and i_2 at the feeding end (i.e. $z = -\infty$). This is because R, the reflection coefficient, is exponentially small and hence is lost in the remainder of the power series arising from the method of solution.

Upon imposing the 3 dB design requirement, exactly as we did before, we get

$$\Delta\beta \sqrt{\frac{\pi}{\alpha}} = \frac{\pi}{4} \tag{30}$$

Eq. (30) is equivalent to (21) but with x exactly equal to $\frac{\pi}{4}$. Consequently, after substituting (26) and (30) in (24) we get

$$d_o = \frac{1}{2h_o} \ln \left[\frac{4c_o^2 R}{h_o}\right] \tag{31}$$

Now, by choosing suitable values for a, b, ε_r, R, and the frequency we will be able to find d_o as well as L(given by Eq. (27)) and hence to plot $i_1(\infty)$ and $i_2(\infty)$ for a full range of frequencies.

IV. Transmission Losses

Thus far, it has been assumed that the two parallel conducting planes had infinite conductivity, and the radii of curvature of the bends were sufficiently large so that radiation losses were negligible. Practical transmission line conductors will have large but finite conductivity and the dielectric will have small but finite conductivity. Approximate attenuation formulas, for the wall and the dielectric losses, were determined by Cohn[7] (For the TE_o even mode) and found to be

$$\alpha_w \, b\sqrt{\lambda_o} = \frac{0.0291}{\sqrt{\sigma_w}} \cdot \left\{ \frac{\pi^2 \varepsilon_r \left(\frac{a}{\lambda_o}\right)^2 - \frac{\left(p_o \frac{a}{2}\right)^2 \cot\left(p_o \frac{a}{2}\right)}{\left(p_o \frac{a}{2}\right) + \cot\left(p_o \frac{a}{2}\right)}}{\left(\frac{a}{\lambda_o}\right)^2 \sqrt{\pi^2 \varepsilon_r \left(\frac{a}{\lambda_o}\right)^2 - \left(p_o \frac{a}{2}\right)^2}} \right\} \tag{32}$$

$$\alpha_d \lambda_o = \frac{\pi^2 \varepsilon_r \, \phi_d \left(\frac{a}{\lambda_o}\right)}{\sqrt{\pi^2 \, \varepsilon_r \left(\frac{a}{\lambda_o}\right)^2 - \left(p_o \frac{a}{2}\right)^2}} \cdot \left[\frac{p_o \frac{a}{2} + \sin\left(p_o \frac{a}{2}\right) \cos\left(p_o \frac{a}{2}\right)}{p_o \frac{a}{2} + \cot\left(p_o \frac{a}{2}\right)} \right] \tag{33}$$

respectively, where α_w , σ_w , α_d , λ_o and ϕ_d are the attenuation due to the wall loss, the wall conductivity, the attenuation due to the dielectric loss, the free space wavelength, and the loss tangent of the dielectric. It is also understood that a and b are, respectively, the width and the height of the dielectric.

The attenuation constant α_R due to radiation, caused by bending the dielectric slab, has been calculated (for the TE_o even mode) by many authors [20-21] and is given by

$$\alpha_R = \frac{h_o \, p_o}{\beta_o \, k_o^2 (\varepsilon_r - 1) \left(a + \frac{2}{h_o}\right)} \, e^{ha - 2\left[\beta_o \tanh^{-1}\left(\frac{h_o}{\beta_o}\right) - h_o\right] R} \tag{34}$$

V. Design and Performance of a 3dB Coupler

The present section gives additional design information, and reports progress toward achieving a tight 3dB wideband dielectric directional coupler.

A typical example of a 3dB coupler, fed symmetrically and antisymmetrically by the TE_o even mode (dominant mode) or by the first hybrid $H_x = o$ mode, is considered. The dimensions of the guides (i.e. a and b) as well as ε_r , are found to have no substantial effect on the flatness of the frequency response.

The frequency response of a 3dB coupler, fed by the dominant mode, and with

$$\begin{aligned} a &= 1.35 \text{ mm} \\ b &= 1.0 \text{ mm} \\ \varepsilon_r &= 2.0 \end{aligned} \tag{35}$$

is shown in Fig. 3. When the dimensions of the guides and ε_r are changed to

$$\begin{aligned} a &= 1.25 \text{ mm} \\ b &= 1.0 \text{ mm} \\ \varepsilon_r &= 2.2 \end{aligned} \tag{36}$$

the frequency response is not substantially altered; as shown in Fig. 4. The values of the attenuation, due to the dielectric losses (with $\phi_d = 0.001$) and due to the wall losses ($\sigma_w = 5.8 \times 10^5 \mho/\text{cm}$), are calculated and found to be of the orders of 10^{-2} neper/cm and 10^{-3} neper/cm respectively. The radiation due to the bending of the dielectric slab is calculated and found to be excessive when the radius R is smaller than 15 mm. A reasonable 3dB - bandwidth, that can be attained by using the dimensions of (36) with

d_o = 0.5 mm, is 20 GHz.

A second case, where the 3dB dielectric coupler is fed by the lowest $H_x = 0$ hybrid mode, is examined. The 3dB bandwidth, compared to the first case, is not so large as illustrated in figure 5.

VI. Conclusions

1. The fields on both lines are closely in quadrature.
2. The reflection coefficient in line 1, and the reverse coupling (directivity) of line 2, are exponentially small and can be neglected.
3. Large losses, due to radiation, are found when the radius of curvature R, of the curved line, is less than 15 mm.
4. The TE_o dominant mode is found to yield better frequency response than the lowest order $H_x = 0$ hybrid mode.
5. A single curved section coupler is found to give better 3dB bandwidth, and negligible reflection and directivity, compared to a curved-linear-curved 3 sections coupler.

References

(1) F.J. Tischer, "A waveguide structure with low losses," Arch. Elek. Übertragung, vol 7, Dec 1953, pp 592-596.

(2) F.J. Tischer, "The H-Guide, a waveguide for microwaves," 1956 IRE Convention Record pt. 5, pp 44-47.

(3) F.J. Tischer, "Properties of the H-Guide at microwaves and millimeter waves," 1958 Wescon Rec., pt. 1, pp 4-12.

(4) F.J. Tischer, "H-Guide with Laminated Dielectric," Proc. IEEE, vol 57, no. 5, pp 820-821, May 1969.

(5) F.J. Tischer, "Fence Guide for Millimeter Waves," Proc. IEEE, vol 59, no 7, pp 1112-1113, July 1971.

(6) M. Cohn, "Parallel Plane Waveguide Partially Filled with a Dielectric," Proc. IRE, vol 46, no. 12, pp 1952-1953, Dec 1958.

(7) M. Cohn, "Propagation in a Dielectric-Loaded Parallel Waveguide," IRE Trans., MTT-7, no. 4, pp 202-208, April 1959.

(8) R. Moore and R. Beam, "A duo-dielectric parallel-plane waveguide," Proc. NEC, vol 12, pp 689-705, April 1957.

(9) B.J. Duncan, L. Swern, and K. Tomiyasu, "Microwave Magnetic Field in Dielectric Loaded Coaxial Line," Proc. IRE, vol 46, no 2, pp 500-501, Feb 1958.

(10) M. Abouzahra and L. Lewin, "Dielectric Image line Coupler," Rept 49, Electromagnetics Laboratory, University of Colorado at Boulder, May 1979.

(11) S.E. Miller, "Coupled wave theory and waveguide applications," BSTJ, vol 33, no 3, pp 661-719, May 1954.

(12) E.A. Marcatili, "Dielectric rectangular waveguide and directional coupler for integrated optics," BSTJ, vol 48, no 7, pp 2071-2102, 1969.

(13) D. Marcuse, "The coupling of degenerate modes in two parallel dielectric waveguides," BSTJ, vol 50, no 6, pp 1791-1816, 1971.

(14) M. Matsuhara and A. Watanbe, "Coupling of curved transmission lines, and application to optical directional couplers," J. Opt. Soc Amer, vol 65, no 2, pp 163-168, Feb. 1975.

(15) L. Anderson, "On the coupling of degenerate modes on non-parallel dielectric waveguides," Microwaves, Opt and Acoustic, vol 3, no 2, March 1979.

(16) T. Itanami and S. Shindo, "Channel Dropping Filter for Millimeter-Wave Integrated Circuits," IEEE Trans on Microwave Theory Tech, vol MTT-26, pp 759-764, Oct 1978.

(17) T.N. Trinh and R. Mittra, "Coupling characteristics of Dielectric Waveguides of Rectangular Cross-section," 1980 IEEE MTT-S International Microwave Symposium Digest, 28-30 May 1980, Washington, D.C., pp 214-217.

(18) M. Abouzahra and L. Lewin, "Coupling of Degenatrate Modes on Curved Dielectric Slab Sections and Application to Directional Couplers," IEEE Trans. Microwave Theory Tech, vol MTT-28, no 10, pp 1096-1101, 1980.

(19) R.E. Collin, Field Theory of Guided Waves, New York, McGraw Hill, chap 6, 1980.

(20) L. Lewin, D.C. Chang and E. Kuester, Electromagnetic Waves and Curved Structures, London, Peter Peregrinus, chap 8, 1977.

(21) D. Marcuse, Light Transmission Optics, New York, Van Nostrand-Reinhold, pp 400-404, 1972.

(22) M. Barnoski, Introduction to Integrated Optics, New York and London, Plenum Press, chapter 11, 1973.

APPENDIX A

The field expressions of the hybrid modes, for a single line in isolation as well as for a line pair fed both symmetrically and anti-symmetrically, will be examined. The coupling coefficient in an infinite parallel line, supporting the lowest order $H_x = 0$ (i.e. LSM) hybrid mode, will be deduced. The factor $e^{j(\omega t - \beta_o z)}$ which is common to each of these expressions, has been eliminated in the interest of brevity.

I. Single Line (See Fig. A-1)

Constructing an expression for the electric Hertzian potential, $\overline{\Pi}_e$, so that it is directed in the x-direction and satisfies the Vector Helmholtz equation, and using the two relations

$$\overline{H} = j\omega\varepsilon_o\varepsilon_r \nabla \times \overline{\Pi}_e$$

and

$$\overline{E} = \nabla \times \nabla \times \overline{\Pi}_e \qquad \text{(A-1)}$$

the field distribution can be calculated. The expressions for the field components of the lowest symmetrical $H_x = 0$ (LSM) hybrid mode are listed below.

Region 1 (Dielectric)

$$\Pi_{ex} = A \cos[n \tfrac{\pi}{b} y]\cos[p_o x] \qquad \text{(A-2)}$$

$$H_x = 0$$

$$H_y = \omega\varepsilon_o\varepsilon_r\beta_o A\cos[n \tfrac{\pi}{b} y] \cos[p_o x]$$

$$H_z = j\omega\varepsilon_o\varepsilon_r[n \tfrac{\pi}{b}] A \sin[\tfrac{n\pi}{b} y] \cos[p_o x]$$

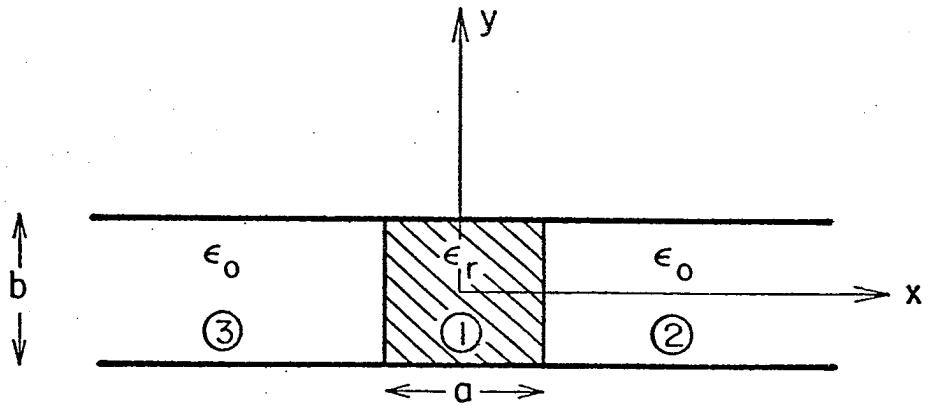

Fig. A-1 Single line in isolation

$$E_x = [\beta_o^2 + (\frac{n\pi}{b})^2]A \cos[\frac{n\pi}{b} y] \cos[p_o x] \tag{A-3}$$

$$E_y = p_o(\frac{n\pi}{b}) A \sin(\frac{n\pi}{b} y) \sin[p_o x]$$

$$E_z = j\beta_o p_o A \cos[\frac{n\pi}{b} y] \sin p_o x$$

where

$$p_o^2 = k_o^2 \varepsilon_r - \beta_o^2 - (\frac{n\pi}{b})^2 \tag{A-4}$$

Region 2 and 3 (Air)

$$\Pi_{ex} = \omega\varepsilon_o\varepsilon_r\beta_o A \cos[p_o \frac{a}{2}] \cos[\frac{n\pi}{b} y] e^{-h_o[|x|-\frac{a}{2}]} \tag{A-5}$$

$$H_x = 0$$

$$H_y = \omega\varepsilon_o\varepsilon_r\beta_o A \cos[p_o\frac{a}{2}] \cos[\frac{n\pi}{b}y] e^{-h_o[|x|-\frac{a}{2}]}$$

$$H_z = j\omega\varepsilon_o\varepsilon_r[\frac{n\pi}{b}]A \cos[p_o\frac{a}{2}] \sin[\frac{n\pi}{b} y] e^{-h_o[|x|-\frac{a}{2}]}$$

$$E_x = [\beta_o^2 + (\frac{n\pi}{b})^2]\varepsilon_r A \cos[p_o \frac{a}{2}] \cos[\frac{n\pi}{b} y] e^{-h_o[|x| -\frac{a}{2}]}$$

$$E_y = \text{sgn}(x) h_o\varepsilon_r(\frac{n\pi}{b}) A\cos[p_o \frac{a}{2}] \sin[\frac{n\pi}{b} y] e^{-h_o[|x| -\frac{a}{2}]}$$

$$E_z = \text{sgn}(x) j\beta_o h_o\varepsilon_r A\cos[p_o \frac{a}{2}] \cos[\frac{n\pi}{b} y] e^{-h_o[|x| -\frac{a}{2}]} \tag{A-6}$$

where

$$h_o^2 = \beta_o^2 - k_o^2 + (\frac{n\pi}{p})^2 \tag{A-7}$$

By means of (A-4) and (A-7), and when $n = 1$, the formula for determining the critical distance between the conducting planes, b_c, which suppresses all the hybrid modes was calculated and found to be

$$b_c \leq \frac{\lambda}{2\sqrt{1 + (h_o/k_o)^2}} \tag{A-7a}$$

Similarly, the cutoff width of the dielectric slab, a_c, which supports only the dominant mod(i.e., the TE_0 mode) is given by

$$\frac{a_c}{\lambda} \leq \frac{1}{2\sqrt{\varepsilon_r - 1}} \tag{A-7b}$$

The transverse propagation constants h_o and p_o are related by

$$p_o^2 + h_o^2 = k_o^2(\varepsilon_r - 1) \tag{A-8}$$

and

$$\tan[p_o \frac{a}{2}] = \frac{h_o \varepsilon_r}{p_o} \tag{A-9}$$

The field expressions for the antisymmetrical $H_x = 0$ hybrid mode, can be extracted from the previous expression by replacing $\cos[p_o x]$ by $\sin[p_o x]$ and $\sin[p_o x]$ by $-\cos[p_o x]$.

II. Two Parallel Lines (See Fig. A-2)

All assumptions used in the previous section hold here. The field region is subdivided into five partial regions. The field expressions for the symmetrical $H_x = 0$ hybrid mode will be listed below.

Region 1

$$\Pi_{ex} = A \cos(n \frac{\pi}{b} y) e^{-hx} \tag{A-10}$$

$$H_x = 0$$

$$H_y = \omega\varepsilon_o \beta A \cos(n \frac{\pi}{b} y) e^{-hx}$$

$$H_z = j\omega\varepsilon_o (\frac{n\pi}{b}) A \sin(n \frac{\pi}{b} y) e^{-hx}$$

$$E_x = [\beta^2 + (n \frac{\pi}{b})^2] A \cos(n \frac{\pi}{b} y) e^{-hx} \tag{A-11}$$

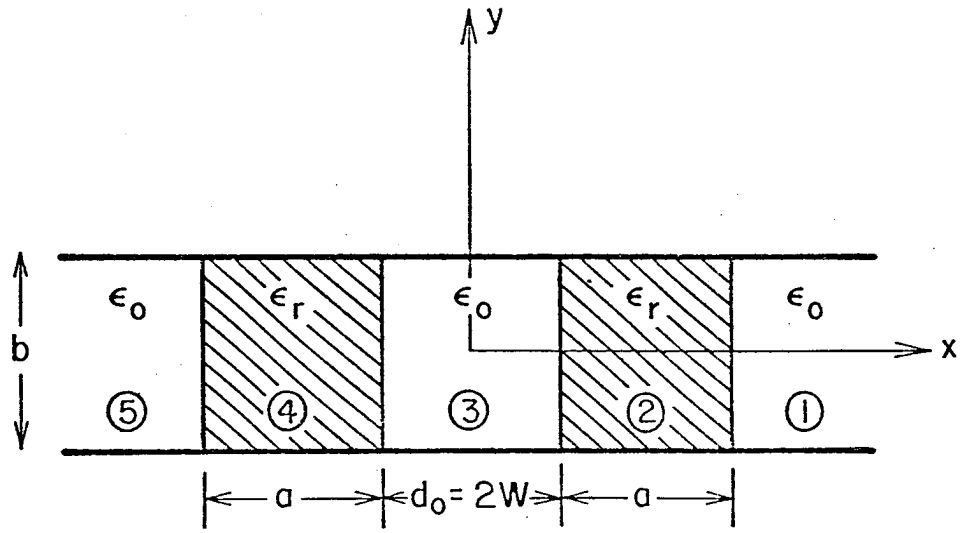

Fig. A-2 Parallel dielectric lines

$$E_y = h\left(\frac{n\pi}{b}\right) A \sin\left(n\frac{\pi}{b}y\right) e^{-hx}$$

$$E_z = j\beta h A \cos\left(n\frac{\pi}{b}y\right) e^{-hx}$$

where

$$h^2 = \beta^2 - k_o^2 + \left(\frac{n\pi}{b}\right)^2 \qquad \text{(A-12)}$$

Region 2

$$\Pi_{ex} = [B \sin(px) + D \cos(px)] \cos\left(n\frac{\pi}{b}y\right) \qquad \text{(A-13)}$$

$$H_x = 0$$

$$H_y = \omega\varepsilon_o\varepsilon_r\beta\,[B \sin(px) + D \cos(px)] \cos\left(\frac{n\pi}{b}y\right)$$

$$H_z = j\omega\varepsilon_o\varepsilon_r\left(\frac{n\pi}{b}\right)[B \sin(px) + D \cos(px)] \sin\left(\frac{n\pi}{b}y\right)$$

$$E_x = \left[\beta^2 + \left(\frac{n\pi}{b}\right)^2\right][B \sin(px) + D \cos(px)]\cos\left(\frac{n\pi}{b}y\right)$$

$$E_y = -p\left(\frac{n\pi}{b}\right)[B \cos(px) - D \sin(px)] \sin\left(\frac{n\pi}{b}y\right)$$

$$E_z = -j\beta p[B \cos(px) - D \sin(px)]\cos\left(\frac{n\pi}{b}y\right) \qquad \text{(A-14)}$$

where

$$p^2 = k_o^2\varepsilon_r - \left(\frac{n\pi}{b}\right)^2 - \beta^2 \qquad \text{(A-15)}$$

Region 3

$$\Pi_{ex} = C \cos\left(n\frac{\pi}{b}y\right) \cosh(hx) \qquad \text{(A-16)}$$

$$H_x = 0$$

$$H_y = \omega\varepsilon_o\beta\, C\cos\left(n\frac{\pi}{b}y\right) \cosh(hx)$$

$$H_z = j\omega\varepsilon_o\left(\frac{n\pi}{b}\right) C\sin\left(n\frac{\pi}{b}y\right) \cosh(hx)$$

$$E_x = [\beta^2 + (n\tfrac{\pi}{b})^2] C \cos(\tfrac{n\pi}{b}y) \cosh(hx) \quad \text{(A-17)}$$

$$E_y = -h (n\tfrac{\pi}{b}) C \sin(\tfrac{n\pi}{b}y) \sinh(hx)$$

$$E_z = -j\beta h C \cos(n\tfrac{\pi}{b}y) \sinh(hx)$$

The field distribution for Regions (4) and (5) is identical to that of regions (1) and (2) but with -y replacing y and different arbitrary constant coefficients.

The arbitrary constant coefficients A,B,C, and D are related in the following fashion, from the boundary conditions,

$$A = -\frac{p}{h}\{B\cos[p(w+a)] - D\sin[p(w+a)]\}e^{h(w+a)} \quad \text{(A-18)}$$

$$C = \frac{P}{h}\left\{\frac{B\cos(pw) - D\sin(pw)}{\sinh(hw)}\right\} \quad \text{(A-19)}$$

$$\frac{B}{D} = \frac{\sin[p(w+a)] - (\frac{h\varepsilon_r}{p})\cos[p(w+a)]}{\cos[p(w+a)] + (\frac{h\varepsilon_r}{p})\sin[p(w+a)]} \quad \text{(A-20)}$$

The characteristic equation is

$$(\frac{p}{h\varepsilon_r})\coth(hw) = \frac{p\cos(pa) + h\varepsilon_r\sin(pa)}{p\sin(pa) - h\varepsilon_r\cos(pa)]} \quad \text{(A-21)}$$

which can be reduced to

$$\frac{h\varepsilon_r}{p}\tanh(hw) = \tan[\frac{p}{h\varepsilon_r}\tan(pa)] \quad \text{(A-22)}$$

The field distributions of the antisymmetrical mode are exactly identical to that of the symmetrical mode apart from replacing sinh(hw) by cosh(hw) and vice versa.

Following the same course of derivation used in Report No. 49, we found that, for the case of $n = 1$, $H_x = 0$ hybrid mode, the coupling coefficient is given by

$$\Delta\beta = \frac{h_o \varepsilon_r p_o^2 \, e^{-2h_o w}}{\beta_o k_o^2 (\varepsilon_r - 1)\left[\frac{a}{2} + \frac{\varepsilon_r}{h_o} + \frac{a h_o^2}{2k_o^2}(\varepsilon_r + 1)\right]} \qquad \text{(A-23)}$$

When strong coupling is considered (that is, d_o is very small), eq. (A-23) becomes less accurate. As an alternative, equations (A-12), (A-15) and (A-22) are programmed and β_s as well as β_a are calculated numerically. Then, using

$$\Delta\beta = \frac{\beta_s - \beta_a}{2}$$

the shift in propagation constant β_o can be determined.

APPENDIX B

By the method of variation of parameters, an exact solution for

$$\frac{d^2I}{dz^2} + \beta^2 I = - MIf(z) \tag{B-1}$$

that satisfies the boundary conditions (i.e. unit incident actual coupled field $i_1(-\infty)$ and matched i_1 and i_2 at $z = \infty$) was found to be

$$I(z) = e^{-j\beta z} + \frac{M}{2j\beta}\left\{e^{-j\beta z}\int_{-\infty}^{z} f(t)\, I(t)\, e^{j\beta t}dt - e^{j\beta z}\int_{\infty}^{z} f(t)\, I(t)\, e^{-j\beta t}dt\right\} . \tag{B-2}$$

Using the method of iteration (i.e., Picard's iteration method), where a solution of order (n) can be expressed in terms of a solution of order (n-1), eq. (B-2) can be rewritten as,

$$I^{(n)}(z) = e^{-j\beta z} + \frac{M}{2j\beta}\left\{e^{-j\beta z}\int_{-\infty}^{z} f(t)\, I^{(n-1)}(t)\, e^{j\beta t}dt - e^{j\beta z}\int_{\infty}^{z} f(t)\, I^{(n-1)}(t)\, e^{-j\beta t}dt\right\}. \tag{B-3}$$

Choosing $e^{-j\beta z}$ to be the zero order solution $I^{(0)}(z)$, then the first order solution $I^{(1)}(z)$ becomes

$$I^{(1)}(z) = e^{-j\beta z} + \frac{M}{2j\beta}\left\{e^{-j\beta z}\int_{-\infty}^{z} f(t)dt - e^{j\beta z}\int_{\infty}^{z} f(t)\, e^{-2j\beta t}dt\right\}. \tag{B-4}$$

Similarly, the second order solution is,

$$I^{(2)}(z) = e^{-j\beta z} + \frac{M}{2j\beta}\left\{e^{-j\beta z}\int_{-\infty}^{z} f(t)\, I^{(1)}(t)\, e^{j\beta t}dt - e^{j\beta z}\int_{\infty}^{z} f(t)\, I^{(1)}(t)\, e^{-j\beta t}dt\right\}. \quad \text{(B-5)}$$

Moreover, $I^{(2)}(\infty)$ becomes

$$I^{(2)}(\infty) = e^{-j\beta z}\left\{1 + \frac{M}{2j\beta}\int_{-\infty}^{\infty} f(t)\, I^{(1)}(t)\, e^{j\beta t}dt\right\} \quad \text{(B-6)}$$

where the integral on the RHS can be evaluated by making use of (B-4) as follows:

$$\int_{-\infty}^{\infty} f(t)\, I^{(1)}(t)\, e^{j\beta t}dt = \int_{-\infty}^{\infty} f(t)\,dt + \frac{M}{2j\beta}\int_{-\infty}^{\infty} f(z)\int_{-\infty}^{z} f(t)dt\,dz - \frac{M}{2j\beta}\int_{-\infty}^{\infty} f(z)e^{2j\beta z}\int_{-\infty}^{z} f(t)\, e^{-2j\beta t}dt\,dz \quad \text{(B-7)}$$

Upon setting

$$f(t) = e^{-\alpha t^2} \quad \text{(B-8)}$$

$$\phi(z) = \int_{-\infty}^{z} f(t)dt \quad \text{(B-9)}$$

$$\phi(z,\pm j\beta) = \int_{\infty}^{z} f(t)e^{\pm 2j\beta t}dt \quad \text{(B-10)}$$

$$M = 2\beta\Delta\beta \quad \text{(B-11)}$$

equation (B-7) reduces to

$$I^{(2)}(\infty) = e^{-j\beta z}\left\{1 - j\Delta\beta[\phi(\infty) - j\Delta\beta\int_{-\infty}^{\infty}\phi'(z)\phi(z)dz + j\Delta\beta\int_{-\infty}^{\infty}\phi'(z,j\beta)\phi(z,-j\beta)dz]\right\} \quad \text{(B-12)}$$

where the prime sign stands for differentiation with respect to z.

Upon the evaluation of the integrals, (B-12) becomes

$$I^{(2)}(\infty)=e^{-j\beta z}\left\{1 - j\Delta\beta\sqrt{\frac{\pi}{\alpha}} - (\Delta\beta)^2\left[\frac{\pi}{2\alpha}(1+e^{-2\beta^2/\alpha}) - j\sqrt{\frac{\pi}{\alpha}}\,\mathrm{Daw}\left(\beta\sqrt{\frac{2}{\alpha}}\right)\right]\right\} \tag{B-13}$$

where

$$\mathrm{Daw}(x) = e^{-x^2}\int_0^x e^{t^2}dt \tag{B-14}$$

$$\phi(\infty) = \int_{-\infty}^{\infty} e^{-\alpha t^2}dt = \sqrt{\frac{\pi}{\alpha}} \tag{B-15}$$

$$\int_{-\infty}^{\infty}\phi(z)\phi'(z)dz = \frac{1}{2}\phi^2(\infty) = \frac{\pi}{2\alpha} \tag{B-16}$$

The last integral, on the RHS of (B-12), was evaluated as follows:

$$\int_{-\infty}^{\infty}\phi'(z,j\beta)\phi(z,-j\beta)dz = \int_{-\infty}^{\infty} e^{-\alpha z^2+2j\beta z}\int_{-\infty}^{z} e^{-\alpha t^2-2j\beta t}dt\,dz \tag{B-17}$$

By setting $t = z + \theta$, completing the square of the variable z, and carrying out the integration over z, eq. (B-17) yields

$$\int_{-\infty}^{\infty}\phi'(z,j\beta)\phi(z,-j\beta)dz = -\sqrt{\frac{\pi}{2\alpha}}\int_0^{\infty} e^{-2\alpha\left[\frac{\theta^2}{4}+j\beta\frac{\theta}{\alpha}\right]}d\theta \tag{B-18}$$

Upon completing the square in the exponential, and substituting by $x = \frac{\theta}{2} + j\frac{\beta}{\alpha}$, (B-18) becomes

$$\int_{-\infty}^{\infty}\phi'(z,j\beta)\phi(z,-j\beta)dz = -\sqrt{\frac{2\pi}{\alpha}}e^{-2\beta^2/\alpha}\int_{j\beta/\alpha}^{\infty} e^{-2\alpha x^2}dx$$

$$= -\sqrt{\frac{2\pi}{\alpha}}e^{-2\beta^2/\alpha}\left[\int_0^{\infty} e^{-2\alpha x^2}dx - \int_0^{j\beta/\alpha} e^{-2\alpha x^2}dx\right] \tag{B-19}$$

Evaluating the first integral, and then setting $x = jy/\sqrt{2\alpha}$, equation (B-19) gives

$$\int_{-\infty}^{\infty} \phi'(z,j\beta)\phi(z,-j\beta)dz = -\frac{\pi}{2\alpha}\, e^{-2\beta^2/\alpha} + j\,\frac{\sqrt{\pi}}{\alpha}\,\mathrm{Daw}\left(\beta\sqrt{\frac{2}{\alpha}}\right) \qquad \text{(B-20)}$$

where $\mathrm{Daw}(x)$ is defined in (B-14).

Similarly, the second order solution of

$$\frac{d^2 i}{dz^2} + \beta^2 i = M\, if(z) \qquad \text{(B-21)}$$

can be deduced from the solution of (B-1) simply by replacing M by $-M$ (or equivalently $\Delta\beta$ by $-\Delta\beta$) in (B-13). Thus,

$$i^{(2)}(\infty) = e^{-j\beta z}\left\{1 + j\Delta\beta\sqrt{\frac{\pi}{\alpha}} - (\Delta\beta)^2\left[\frac{\pi}{2\alpha}\left(1 + e^{-2\beta^2/\alpha}\right) - j\,\frac{\sqrt{\pi}}{\alpha}\,\mathrm{Daw}\left(\beta\sqrt{\frac{2}{\alpha}}\right)\right]\right\}. \qquad \text{(B-22)}$$

But the actual coupled fields are given by

$$\begin{aligned} i_1^{(2)}(\infty) &= \left[I^{(2)}(\infty) + i^{(2)}(\infty)\right]/2 \\ i_2^{(2)}(\infty) &= \left[I^{(2)}(\infty) - i^{(2)}(\infty)\right]/2 \end{aligned} \qquad \text{(B-23)}$$

and hence

$$i_1^{(2)}(\infty) = e^{-j\beta z}\left\{1 - (\Delta\beta)^2\left[\frac{\pi}{2\alpha}\left(1 + e^{-2\beta^2/\alpha}\right) - j\,\frac{\sqrt{\pi}}{\alpha}\,\mathrm{Daw}\left(\beta\sqrt{\frac{2}{\alpha}}\right)\right] + 0(\Delta\beta)^4\right\} \qquad \text{(B-24)}$$

$$i_2^{(2)}(\infty) = - j\Delta\beta\sqrt{\frac{\pi}{\alpha}}\, e^{-j\beta z} \tag{B-25}$$

Up to the current order of accuracy, and for small $\Delta\beta$, it is already clear that $i_1(\infty)$ and $i_2(\infty)$ are in quadrature.

Following closely, the previous course of derivation, $i_1^{(2)}(-\infty)$ and $i_2^{(2)}(-\infty)$ are calculated and found to be

$$i_1^{(2)}(-\infty) = e^{-j\beta z} - (\Delta\beta)^2\, e^{j\beta z}\{\frac{\pi}{\alpha}\, e^{-\beta^2/\alpha} - 2j\,\frac{\sqrt{\pi}}{\alpha}\, e^{-\beta^2/2\alpha} \cdot \mathrm{Daw}(\frac{\beta}{\sqrt{2\alpha}})\} \tag{B-26}$$

$$i_2^{(2)}(-\infty) = -j\Delta\beta\,\sqrt{\frac{\pi}{\alpha}}\, e^{-\beta^2/\alpha}\, e^{j\beta z} \tag{B-27}$$

which means that

$$R^{(2)}(-\infty) = - (\Delta\beta)^2\,\{\frac{\pi}{\alpha}\, e^{-\beta^2/\alpha} - 2j\,\frac{\sqrt{\pi}}{\alpha}\, e^{-\beta^2/2\alpha}\,\mathrm{Daw}(\frac{\beta}{\sqrt{2\alpha}})\} \tag{B-28}$$

and

$$D^{(2)}(-\infty) = - j\Delta\beta\sqrt{\frac{\pi}{\alpha}}\, e^{-\beta^2/\alpha} \tag{B-29}$$

By performing one more iteration, the third order solution $I^{(3)}(\infty)$ was found to take the form

$$I^{(3)}(\infty) = I^{(2)}(\infty) + j(\Delta\beta)^3[Q_1^+ - Q_2^+ - Q_3^+ + Q_4^+]\, e^{-j\beta z} \tag{B-30}$$

where $I^{(2)}(\infty)$ is given in (B-13), and

$$Q_1^+ = \int_{-\infty}^{\infty} f(t) \int_{-\infty}^{t} f(z) \int_{-\infty}^{z} f(x)\ dx\, dz\, dt \tag{B-31}$$

$$Q_2^+ = \int_{-\infty}^{\infty} f(t) \int_{-\infty}^{t} f(z)e^{2j\beta z} \int_{\infty}^{z} f(x)e^{-2j\beta x}\, dx\, dz\, dt \tag{B-32}$$

$$Q_3^+ = \int_{-\infty}^{\infty} f(t)e^{2j\beta t} \int_{\infty}^{t} f(z)e^{-2j\beta z} \int_{-\infty}^{z} f(x)\, dx\, dz\, dt \tag{B-33}$$

$$Q_4^+ = \int_{-\infty}^{\infty} f(t)e^{2j\beta t} \int_{\infty}^{t} f(z) \int_{\infty}^{z} f(x)e^{-2j\beta x}\, dx\, dz\, dt \tag{B-34}$$

The above integrals are similar to those of (B-16) and (B-17), and hence can be evaluated in a similar fashion. These integrals were evaluated and found to be

$$Q_1^+ = \frac{1}{6}\left(\frac{\pi}{\alpha}\right)^{3/2} \tag{B-35}$$

$$Q_2^+ = Q_3^+ = -\frac{\pi}{2\alpha}\sqrt{\frac{3}{\alpha}}\; e^{-2\beta^2/\alpha} \int_0^{\infty} e^{-3\left[x + j\beta\sqrt{\frac{2}{3\alpha}}\right]^2} [1 + \operatorname{erf}(x)]dx \tag{B-36}$$

$$Q_4^+ = \frac{\pi}{2\alpha}\sqrt{\frac{3}{\alpha}}\; e^{-2\beta^2/\alpha} \int_0^{\infty} e^{-3\left[x + j\frac{\beta}{\sqrt{6\alpha}}\right]^2} \operatorname{erfc}\left[x + j\beta\sqrt{\frac{3}{2\alpha}}\right]dx \tag{B-37}$$

The two integrals Q_2^+ and Q_3^+ were found to be equal, despite the fact that (B-32) and (B-33) do not look the same. Similarly $I^{(3)}(-\infty)$ was calculated and found to be as follows:

$$I^{(3)}(-\infty) = I^{(2)}(-\infty) + j(\Delta\beta)^3[Q_1^- - Q_2^- - Q_3^- + Q_3^-]e^{j\beta z} \tag{B-38}$$

where $I^{(2)}(-\infty)$ is given before (half the sum of (B-26) and (B-27)) and

$$Q_1^- = \int_{-\infty}^{\infty} f(t)\; e^{-2j\beta t} \int_{-\infty}^{t} f(z) \int_{-\infty}^{z} f(x)\, dx\, dz\, dt \tag{B-39}$$

$$Q_2^- = \int_{-\infty}^{\infty} f(t)e^{-2j\beta t} \int_{-\infty}^{t} f(z)e^{2j\beta z} \int_{\infty}^{z} f(x)e^{-2j\beta x}\, dx\, dz\, dt \tag{B-40}$$

$$Q_3^- = \int_{-\infty}^{\infty} f(t) \int_{\infty}^{t} f(z) e^{-2j\beta z} \int_{-\infty}^{z} f(x)\, dx\, dz\, dt \tag{B-41}$$

$$Q_4^- = \int_{-\infty}^{\infty} f(t) \int_{\infty}^{t} f(z) \int_{\infty}^{z} f(x) e^{-2j\beta x}\, dx\, dz\, dt \tag{B-42}$$

These integrals were evaluated and found to be

$$Q_1^- = \frac{\pi}{2\alpha}\sqrt{\frac{3}{\alpha}}\, e^{-\beta^2/\alpha} \int_{o}^{\infty} e^{-3x^2}\, \mathrm{erfc}[x + j\beta\sqrt{\frac{2}{3\alpha}}]dx \tag{B-43}$$

$$Q_2^- = -\frac{\pi}{2\alpha}\sqrt{\frac{3}{\alpha}}\, e^{-3\beta^2/\alpha} \int_{o}^{\infty} e^{-3(x+j\beta\sqrt{\frac{2}{3\alpha}})^2} \{1 + \mathrm{erf}[x - j\beta\sqrt{\frac{2}{3\alpha}}]\}dx \tag{B-44}$$

$$Q_3^- = -\frac{\pi}{2\alpha}\sqrt{\frac{3}{\alpha}}\, e^{-\beta^2/\alpha} \int_{o}^{\infty} e^{-3[x+j\frac{\beta}{\sqrt{6\alpha}}]^2} \{1+\mathrm{erf}(u - j\frac{\beta}{\sqrt{6\alpha}})\}\, dx \tag{B-45}$$

$$Q_4^- = \frac{\pi}{2\alpha}\sqrt{\frac{3}{\alpha}}\, e^{-\beta^2/\alpha} \int_{o}^{\infty} e^{-3[x-j\frac{\beta}{\sqrt{6\alpha}}]^2}\, \mathrm{erfc}[u-j\frac{\beta}{\sqrt{6\alpha}}]dx \tag{B-46}$$

Keeping in mind that $i^{(3)}(\infty)$ and $i^{(3)}(-\infty)$ have expressions identical to that of $I^{(3)}(\infty)$ and $I^{(3)}(-\infty)$, apart from replacing M by -M, $i_1(\infty)$, $i_2(\infty)$, $i_1(-\infty)$, and $i_2(-\infty)$ were evaluated and found to be

$$i_1(\infty) = e^{-j\beta z}\left\{1 - (\Delta\beta)^2[\frac{\pi}{2\alpha}(1 + e^{-2\beta^2/\alpha}) - j\frac{\sqrt{\pi}}{\alpha}\mathrm{Daw}(\beta\sqrt{\frac{2}{\alpha}})] + \hat{A}(\Delta\beta)^4\right\} \tag{B-47}$$

$$i_2(\infty) = -j\Delta\beta\sqrt{\frac{\pi}{\alpha}}\, e^{-j\beta z}\left\{1 - (\Delta\beta)^2\frac{\pi}{6\alpha}[1 + \hat{J}_1 + \hat{J}_2]\right\} + O(\Delta\beta)^5 \tag{B-48}$$

$$i_1(-\infty) = e^{-j\beta z} - (\Delta\beta)^2\, e^{j\beta z}\left\{\frac{\pi}{\alpha}e^{-\beta^2/\alpha} - j\frac{2\sqrt{\pi}}{\alpha}e^{-\beta^2/2\alpha}\mathrm{Daw}(\frac{\beta}{\sqrt{2\alpha}})\right\} + O(\Delta\beta)^4 \tag{B-49}$$

$$i_2(-\infty) = -je^{j\beta z}\left\{\Delta\beta\left[\sqrt{\frac{\pi}{\alpha}}\ e^{-\beta^2/\alpha} - (\Delta\beta)^2 \mathrm{Re}(\hat{S})\right] - j(\Delta\beta)^3 \mathrm{Im}(\hat{S})\right\} + O(\Delta\beta)^5 \tag{B-50}$$

where

$$\hat{J}_1 = -\left(\frac{12\alpha}{\pi}\right) Q_2^+ \tag{B-51}$$

$$\hat{J}_2 = \left(\frac{6\alpha}{\pi}\right) Q_4^+$$

$$\hat{S} = \hat{J}_3 + \hat{J}_4 + \hat{J}_5 + \hat{J}_6 \tag{B-52}$$

$$\hat{J}_3 = Q_1^- \tag{B-53}$$

$$\hat{J}_4 = -Q_2^-$$

$$\hat{J}_5 = -Q_3^-$$

$$\hat{J}_6 = Q_4^-$$

$\mathrm{Re}(\hat{A})$ can be evaluated by imposing the law of conservation of energy which is,

$$|i_1(\infty)|^2 + |i_2(\infty)|^2 + |R(-\infty)|^2 + |D(-\infty)|^2 = 1 \tag{B-54}$$

where $R(-\infty)$ and $D(-\infty)$, the reflection coefficient due to coupling and the directivity, are the amplitudes of the reflected wave in the expressions of $i_1(-\infty)$ and $i_2(-\infty)$ respectively. $\mathrm{Re}(\hat{A})$ was evaluated and found to be given by

$$\mathrm{Re}(\hat{A}) = \frac{\pi^2}{6\alpha^2}\left[1 + \mathrm{Re}(\hat{J}_1 + \hat{J}_2)\right] + \sqrt{\frac{\pi}{\alpha}}\, e^{-\beta^2/\alpha}\, \mathrm{Re}(\hat{S})$$

$$- \frac{1}{2}\left[|\hat{K}|^2 + |\hat{C}|^2\right] \qquad \text{(B-55)}$$

where

$$\hat{K} = \frac{\pi}{2\alpha}\left(1 + e^{-2\beta^2/\alpha}\right) - j\sqrt{\frac{\pi}{\alpha}}\ \mathrm{Daw}\left(\beta\sqrt{\frac{2}{\alpha}}\right) \qquad \text{(B-56)}$$

$$\hat{C} = \frac{\pi}{\alpha}\, e^{-\beta^2/\alpha} - j\frac{2\sqrt{\pi}}{\alpha}\, e^{-\beta^2/2\alpha}\, \mathrm{Daw}\left(\frac{\beta}{\sqrt{2\alpha}}\right) \qquad \text{(B-57)}$$

where $\hat{J}_1$, $\hat{J}_2$ and $\hat{S}$ are given in eqs. (B-51) through (B-53).

APPENDIX C

The differential equation that evolved from the transmission line equations take the general form

$$\frac{d^2I}{dz^2} + \beta_o^2 I = -MIf(z) \qquad (C\text{-}1)$$

$$\frac{d^2i}{dz^2} + \beta_o^2 i = Mif(z) \qquad (C\text{-}2)$$

where, I and i are the symmetrical and the antisymmetrical modes of the coupled system, and f(z) is a function of z that appears because of the variable coupling between the curved transmission lines. The general form of f(z) will be considered as $e^{-\alpha z^{2n}}$.

A solution for (C-2), that satisfies the boundary conditions (i.e. unit incident wave at $z = -\infty$ and zero reflected wave at $z = +\infty$) and contains, implicitly, the forward and the backward waves, takes the form

$$i(z) = e^{-j\left[\beta_o z + \int_{-\infty}^{z} g(x)dx\right]} \qquad (C\text{-}3)$$

Then,

$$\frac{di(z)}{dz} = -j\left[\beta_o + g(z)\right] i(z) \qquad (C\text{-}4)$$

$$\frac{d^2i(z)}{dz^2} = -\left[\beta_o + g(z)\right]^2 i(z) - j\frac{d}{dz}\left[g(z)\right] i(z) \qquad (C\text{-}5)$$

For simplification we will write $g(z)$, $f(z)$, and $i(z)$ as g, f, and i respectively. Moreover, the prime will be used to represent the derivative. Thus, from (C-3) and (C-5) we obtain,

$$i'' + \beta_o^2 i = -[\beta_o+g]^2 i - jg'i + \beta_o^2 i = Mif \tag{C-7}$$

and hence

$$g = -\frac{1}{2\beta_o}[Mf+jg'+g^2] \tag{C-8}$$

Let

$$g_1 = -\frac{M}{2\beta_o} f \tag{C-9}$$

when (C-9) is substituted in (C-8) as a first iteration, we get

$$g_2 = -\frac{1}{2\beta_o}\left[Mf-j\frac{M}{2\beta_o} f'+\left(\frac{M}{2\beta_o}\right) f^2\right] \tag{C-10}$$

Upon substituting for g on the RHS of (C-8), we obtain

$$g_3 = -\frac{M}{2\beta_o} f + j\frac{M}{(2\beta_o)} f' - j\frac{M}{(2\beta_o)^3} f'' + 4j\frac{M^2}{(2\beta)^4} ff'$$

$$-\frac{M^2}{(2\beta_o)^3} f^2 + \frac{M^2}{(2\beta_o)^5} f'^2 - \frac{M^4}{(2\beta_o)^7} f^4$$

$$-\frac{2M^3}{(2\beta_o)^5} f^3 + 2j\frac{M^3}{(2\beta_o)^6} f'f^2 \tag{C-11}$$

Assuming

$$f = e^{-\alpha z^{2n}} \tag{C-12}$$

and

$$S = \int_{-\infty}^{\infty} g(x)dx \tag{C-13}$$

then,

$$i(\infty) = e^{-j[\beta z+S]} \tag{C-14}$$

Moreover, according to our problem, M is given by

$$M = 2\beta_o \Delta\beta \tag{C-15}$$

and $2\Delta\beta$ is very small compared to β_o . Therefore, upon carrying the integration of (C-13) (for S_3) and dropping all the small terms, S_3 reduces to

$$S_3 = -\frac{\Delta\beta}{\frac{1}{n\alpha^{2n}}}\Gamma\left(\frac{1}{2n}\right) - \frac{(\Delta\beta)^2}{\frac{1}{n(2\alpha)^{2n}}}\Gamma\left(\frac{1}{2n}\right) \tag{C-16}$$

where $\Gamma(x)$ represents the Gamma function. When $n = 1$ (C-16) reduces to

$$S_3 = -\Delta\beta\sqrt{\frac{\pi}{\alpha}} - \frac{(\Delta\beta)^2}{2\beta_o}\sqrt{\frac{\pi}{2\alpha}} \tag{C-17}$$

and therefore,

$$i(\infty) = e^{-j\beta z}e^{-jS_3} \tag{C-18}$$

As a result of the similarity between (C-1) and C-2), I(z) will have a solution identical to that of i(z) but with M replaced by -M (i.e. $\Delta\beta$ by $-\Delta\beta$), and hence

$$I(\infty) = e^{-j\beta Z}\, e^{j\left[-\Delta\beta\sqrt{\frac{\pi}{\alpha}} + \frac{(\Delta\beta)^2}{2\beta_o}\sqrt{\frac{\pi}{\alpha}}\right]} \qquad (C\text{-}19)$$

consequently

$$i_{1,2}(\infty) = \frac{I(\infty)\pm i(\infty)}{2} \qquad (C\text{-}20)$$

from which it follows that

$$i_1(\infty) = e^{-j\beta_o z}\, e^{j\frac{(\Delta\beta)^2}{2\beta_o}\sqrt{\frac{\pi}{\alpha}}} \cos\left[\Delta\beta\sqrt{\frac{\pi}{\alpha}}\right] \qquad (C\text{-}21)$$

$$i_2(\infty) = -je^{-j\beta_o z}\, e^{j\frac{(\Delta\beta)^2}{2\beta_o}\sqrt{\frac{\pi}{\alpha}}} \sin\left[\Delta\beta\sqrt{\frac{\pi}{\alpha}}\right] \qquad (C\text{-}22)$$

Equations (C-21) and C-22) illustrate, clearly, that $i_1(\infty)$ and $i_2(\infty)$ are in quadrature.

It can be easily shown that when $n = 2$ is substituted in (C-16), identical performance (to the case when $n = 1$) will be achieved but with a smaller α (i.e. larger R and L).